

DEEPWATER PIPELINES: RELIABILITY OF FINITE ELEMENT MODELS IN THE PREDICTION OF COLLAPSE AND COLLAPSE PROPAGATION LOADS

Rita G. Toscano

Center for Industrial Research (CINI)
TENARIS
Argentina
rtoscano@tenaris.com

Eduardo N. Dvorkin

Center for Industrial Research (CINI),
TENARIS
Argentina
edvorkin@tenaris.com

ABSTRACT

In the design of pipelines it is of utmost importance to use validated numerical tools, usually finite element models, to reliably determine the structural limit loads. Also for steel pipes manufacturers it is very important, for establishing the set-up of their production processes, to be able to analyze using validated finite element models the effect that different manufacturing imperfections have on the pipe limit loads (e.g. "ovalization" of the external diameter, eccentricity, residual stresses, etc.)

For deepwater pipelines the most relevant limit states that need to be analyzed are the collapse and collapse propagation under different combinations of external pressure and bending.

In the second section of this paper we discuss the finite element models that we developed to predict the collapse and collapse propagation of seamless steel pipes under external pressure and bending. The validation of these models was performed comparing the numerical results with experimental results obtained at C-FER (Edmonton, Canada) [1] and at our lab for the pre-collapse and post-collapse regimes.

In deepwater pipelines, in order to prevent the propagation of collapse failures through the pipeline length, buckle arrestors are used.

In the third section of this paper we review the finite element models that we developed to predict buckle arrestors cross-over external pressures. The validation of these models was performed comparing the numerical results with experimental ones obtained at our lab for different ratios [arrestor thickness/pipe thickness] corresponding to either the flattening or flipping cross-over mechanisms [2].

Finally in the fourth section of this paper the validated finite element models are used to perform parametric analyses that provide useful data for pipeline engineers on the effect of different geometrical parameters on crossover pressure.

INTRODUCTION

In the design of marine pipelines it is fundamental to be able to determine the collapse pressure of steel pipes subjected

to external hydrostatic pressure and bending and it is required to be able to quantify the effect of manufacturing imperfections such as ovality, eccentricity and residual stresses on the collapse pressure.

The tracking of the post-collapse equilibrium path (e.g. the external pressure/internal volume curve) is also necessary in order to assess on the stability of the post-collapse regime; that is to say, in order to assess if a collapse will be localized in a section or will propagate along the pipeline. Hence, it is also required to be able to analyze the effect of the geometrical imperfections and of the residual stresses on the collapse propagation pressure, which is the lowest external pressure that will propagate the collapse along the pipeline, for a constant applied curvature.

The finite element method is an adequate and reliable tool for the above mentioned studies [1, 3-6].

If by accident the collapse is initiated at a certain location, the collapse is either restrained to the collapse initiation section or it propagates along the pipeline, being this second alternative the most detrimental one for the pipeline integrity [7]. Since the external collapse propagation pressure is quite low in comparison with the external collapse pressure, it is necessary to build in the pipeline periodic reinforcements, usually steel rings, to arrest a possible collapse propagation.

Two different buckle arrestor cross-over mechanisms were identified in the literature: flattening and flipping. The occurrence of either cross-over mechanism is determined by the geometry of the pipes and of the arrestors [2].

In this paper we present finite element models to analyze the collapse pressure, collapse propagation pressure and cross-over pressure of pipelines and we discuss the experimental verification of these models: we compare finite element results with experimental ones for full-scale collapse tests under external pressure, external pressure followed by bending and bending followed by external pressure.

The test programs were performed at C-FER Technologies (C-FER), in Canada and at CINI, in Argentina, using TENARIS steel seamless pipes [1]; while the finite

element analyses were performed by CINI, using the general-purpose finite element code ADINA [8].

The numerical / experimental comparisons reported in this paper demonstrate a very good agreement between the finite element predictions and the laboratory observations.

COLLAPSE AND POST-COLLAPSE REGIME

The experimental program

The testing involved performing material property tests, initial geometry measurements, full-scale P tests (collapse and post-collapse under external pressure only), full-scale P→B tests (external pressure first, then increase bending up to collapse), and a full-scale B→P test (bending first, then increase external pressure up to collapse) on steel seamless pipe samples.

Nine samples were tested, all of them conforming to API 5L grade X65. The nominal dimensions for each sample are indicated in Table 1.

| Sample | Nominal OD [mm] | Nominal wall thickness [mm] | Test |
|--------|-----------------|-----------------------------|------|
| 1 | 353 | 22 | P |
| 2 | 353 | 22 | P→B |
| 3 | 353 | 22 | P→B |
| 4 | 323.85 | 17.65 | P |
| 5 | 323.85 | 17.65 | P→B |
| 6 | 323.85 | 17.65 | P→B |
| 7 | 323.85 | 20.30 | P |
| 8 | 323.85 | 20.30 | P→B |
| 9 | 323.85 | 20.30 | B→P |

Table 1. Tested samples

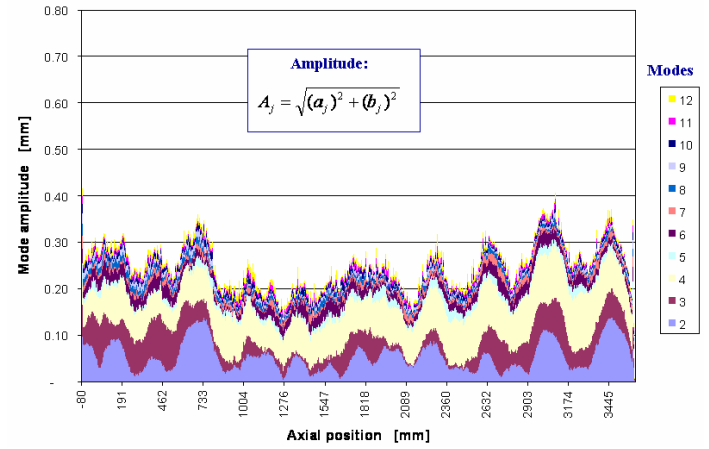
Geometrical characterization of the specimens

Geometric measurements were performed at CINI using:

- Manual ultrasonic gages for mapping the wall thickness at a number of points evenly distributed on the sample external surfaces.
- The shapemeter, described in Ref. [3], for acquiring a detailed description of the pipes OD.

Using the shapemeter a “best fit circle” is determined for transversal sections closely spaced (approx. 2 mm apart) and for each section the deviations between the actual radius at each point and the section “best fit radius” are plotted as a function of the polar angle: $f(\vartheta)$. A Fourier decomposition of $f(\vartheta)$ is then performed [3].

In Figure 1 a detail of the $f(\vartheta)$ Fourier decomposition is presented: a typical amplitude distribution is represented as a function of the axial position along the pipe. Fig. 2 shows a typical thickness distribution.



Algorithm to process the data acquired with the shapemeter

$$r(\vartheta) = R_0 + \sum_{j=1}^N [a_j \cdot \cos(j\vartheta) + b_j \cdot (j\vartheta)] \quad (1)$$

(R_0 is the best-fit circle)

Figure 1. Acquisition of the actual OD “shape”. Shapemeter.

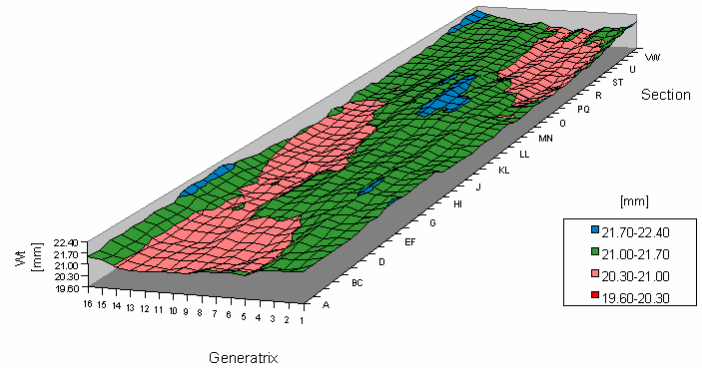


Figure 2. Typical thickness distribution.

Here it is important to introduce some remarks:

- The imperfection mode that controls the value of the buckling pressure is the second one [3].
- The angular orientation of the second mode at each section has an important influence on the collapse pressure. When the ellipse that characterizes the second mode is rotated from one section to the next one, the collapse pressure is higher than for the case of aligned ellipses [3].
- The value of that second mode is quite different (lower) from the ovality measured with a standard API ovalimeter [9].

Mechanical characterization of the specimens

On longitudinal and circumferential coupons, the yield stress and hardening properties of the specimens steel were determined.

Using the standard slit ring test [3] the sample hoop residual stresses were determined.

Full-scale tests

C-FER Deepwater Experimental Chamber was used for all the full-scale tests. The chamber, shown in Fig. 3, has a tested pressure capacity of 62 MPa [9000 psi], with an inside diameter of 1.22 m and an overall inside length of 10.3 m.



Figure 3. C-FER Deepwater Collapse Chamber

Three collapse and buckle propagation tests were conducted. Two of the collapse tests required pressures in excess of 62 MPa [9000]. To achieve higher pressures, a secondary pressure vessel was used inside of the Deepwater Experimental Chamber, allowing pressures up to 80 MPa [11600 psi]. After initial collapse, continuing to pump water into the pressure vessel propagated the buckle.

A detailed description of the experimental procedures was presented in Ref. [1].

The Finite Element Analysis

In previous publications CINI presented finite element models that simulate the collapse and post-collapse behavior of steel pipes under external pressure and bending. Those finite element models were used to analyze the effect of different imperfections on the collapse pressure and on the collapse propagation pressure of the steel pipes [1-3-6].

The finite element models were developed using a material and geometrical nonlinear formulation [10] and they incorporate the following features:

- Geometry as described by the OD mapping and by the thickness distribution measured as reported above.
- MITC4 shell element [11-13].
- Von Mises elastic - perfectly plastic material model with the yield stress corresponding to the samples hoop yield stress in compression. In this model the plastic anisotropy of the material is neglected.
- Circumferential residual stresses as reported above.
- Contact elements on the pipe inner surface [10] in order to prevent its inter-penetration in the post-collapse regime.
- Nonlinear equilibrium path tracking via the algorithm described in Ref. [14].

In what follows, in order to validate the numerical models, for the nine tests described in Table 1 we compare the finite element results with the full-scale test results.

Comparison between numerical and experimental results

In Fig. 4, we compare the experimentally and numerically determined [External Pressure vs. Internal Volume Reduction] diagrams, for the pipes under external pressure only (P- Tests).

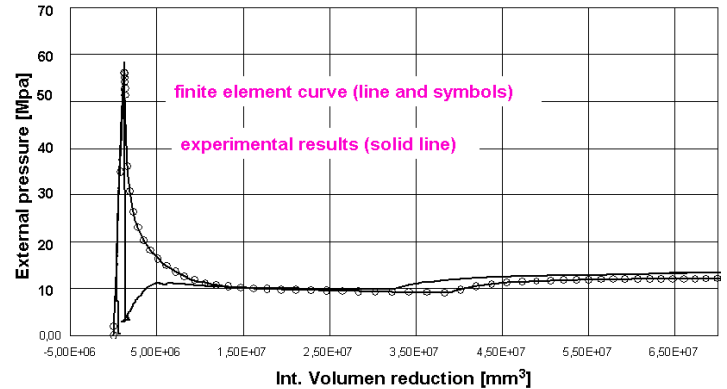


Figure 4. Sample 4, external pressure vs. internal volume reduction; finite element curve and experimental results.

Both curves are practically coincident, except in the interval that goes from immediately after the pipe collapse to the point at which the experimentally and numerically determined curves merge again. In the experimental test, after collapse the chamber is abruptly depressurized and water must be pumped to regain pressure. Hence, the [External Pressure vs. Internal Volume Reduction] experimental path is different from the numerical one, which better represents the undersea conditions. From tests 1 and 7 we obtained similar results.

In Fig. 5, for the same sample shown in Fig. 4, we can observe the deformed meshes for different load points, and a photograph of the collapsed pipe.

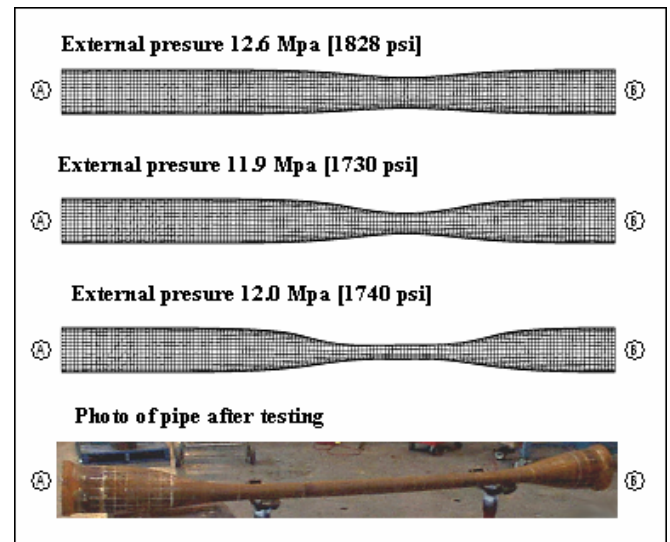


Figure 5. Test 1, deformed meshes and final pipe shape.

From the presented results we can assess that the post-collapse response of the finite element model, specifically the path in which the collapse propagates, has an excellent match with the experimental results.

The raising part of the collapse pressure in the post-collapse regime is due to the contact between points on the pipe inner surface (e.g. the pressure raises from 10 MPa [1450 psi] to approximately 12 MPa [1740 psi] which is the pipe propagation pressure)

For the P→B Tests the 5 samples were first loaded with external pressure and afterwards, maintaining constant the external pressure, they were bent up to collapse.

The ninth sample (B→P Tests) was bent up to a maximum bending strain of 1.33% and afterwards, maintaining the bending strains constant, it was loaded with an increasing external pressure up to collapse.

In the following table we compare the numerical and experimental results:

| Sample | Test | | Numerical results/ Experimental results |
|--------|------|-------------------------------|--|
| 1 | P | Collapse pressure | 0.977 |
| | | Collapse propagation pressure | 0.87 |
| 2 | P→B | Collapse bending | 1.047 |
| 3 | P→B | Collapse bending | 1.088 |
| 4 | P | Collapse pressure | 0.966 |
| | | Collapse propagation pressure | 0.89 |
| 5 | P→B | Collapse bending | 0.972 |
| 6 | P→B | Collapse bending | 0.998 |
| 7 | P | Collapse pressure | 1.103 |
| | | Collapse propagation pressure | 0.99 |
| 8 | P→B | Collapse bending | 0.998 |
| 9 | B→P | Collapse pressure | 0.964 |

Table 2. Numerical vs. experimental results

BUCKLE ARRESTORS: CROSS-OVER EXTERNAL PRESSURE

Experimental results using seamless pipes

Few experimental results are available in the literature for the cross-over of integral ring buckle arrestors under external pressure on large diameter carbon steel pipes [15, 16]. Most of the available experimental results correspond to stainless steel and small diameter steel pipes [2, 17-19].

The purpose of our laboratory tests was to determine the equilibrium path for the assembly (pipe + arrestor + pipe) under external pressure; and from it determine the collapse pressure, the propagation pressure and the cross-over pressure. Fig. 6 shows the experimental assembly.

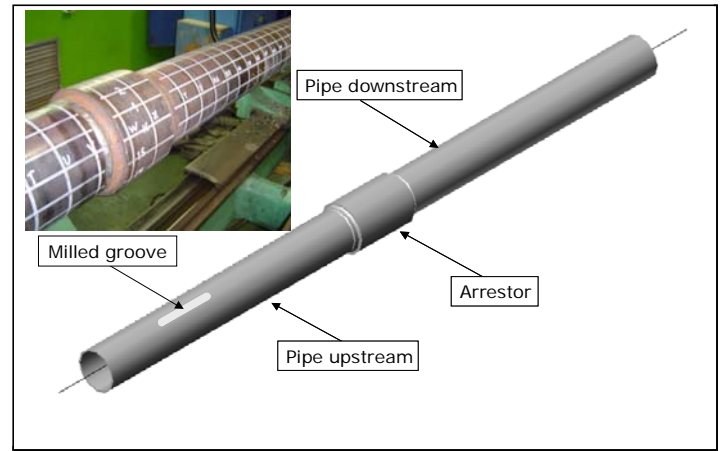


Figure 6. Experimental set-up

To localize the buckle initiation we milled a groove in one of the pipes (upstream pipe). In Fig. 7 we present a detail of the arrestors:

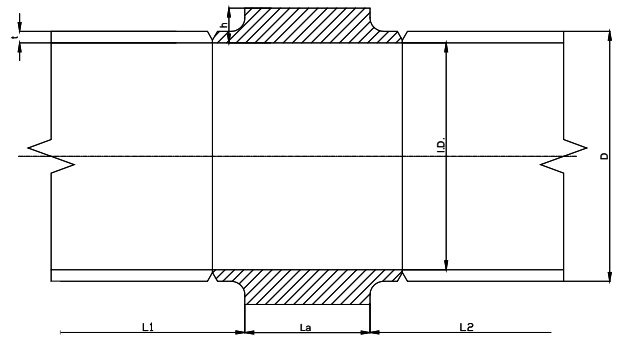


Figure 7. Arrestor geometry

Table 3 provides the data for the tested samples:

| Sample | Pipe OD [mm] | Pipe thickness (t) [mm] | Pipe steel grade | Arrestor (h/t) | Arrestor (La/D) | Arrestor steel grade | Sample length [mm] | Expected cross-over mechanism [2] |
|--------|--------------|-------------------------|------------------|----------------|-----------------|----------------------|--------------------|-----------------------------------|
| 1 | 141.3 | 6.55 | X42 | 2.0 | 0.50 | 6 (ASTM A-333) | 2250 | Flattening |
| 2 | 141.3 | 6.55 | X42 | 2.5 | 0.50 | X42 | 2250 | Flattening |
| 3 | 141.3 | 6.55 | X42 | 3.0 | 0.75 | X42 | 2274 | Flipping |
| 4 | 141.3 | 6.55 | X42 | 3.0 | 1.00 | X42 | 2330 | Flipping |

Table 3. Data for tested samples

Geometrical Characterization of the Tested Samples

The outer surface of the samples was mapped using the shapemeter [3]; the corresponding Fourier decomposition of one of the tested samples is shown in Fig. 8. The zone with high amplitude correspond to the milled groove, whereas the zone with low amplitude belong to the arrestor, which was machined in a lathe.

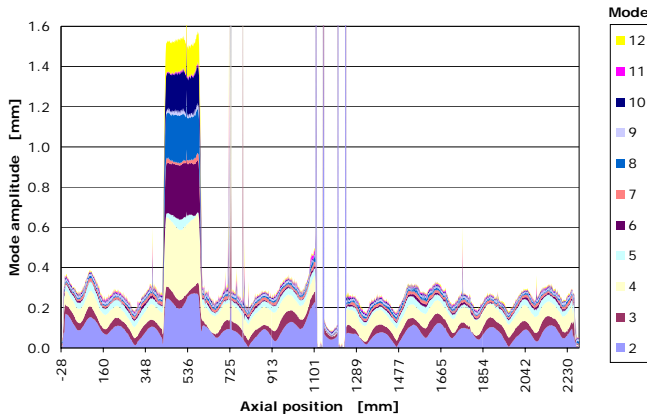


Figure 8. OD Fourier analysis of the first sample

The thickness of the samples were also mapped using a standard ultrasonic gauge; the corresponding thickness map of the first sample is shown in Fig. 9.

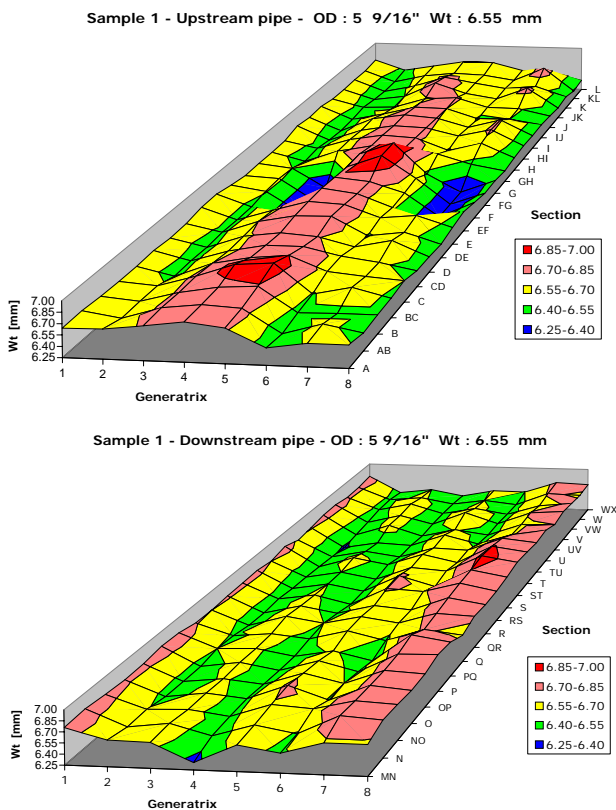


Figure 9. Thickness distribution for the first sample

Mechanical Characterization of the Tested Samples

For all the pipe and arrestor materials we determined:

- True stress – true strain curves (tensile test)
- Hoop residual stresses (slit ring test)

Experimental facility

In Fig. 10 we present a scheme of the experimental set-up. In order to measure the internal volume variation perforated end-caps were welded to the pipes. Each specimen was completely filled with water before the test started. From the hole in one of the end caps the water was directed to a container connected to a load cell. The load variation in the load cell is proportional to the displaced water.

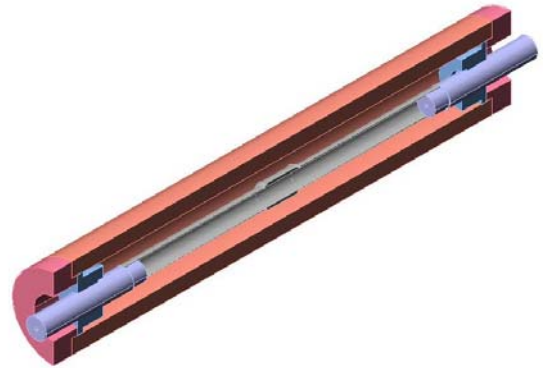


Figure 10. Experimental set-up

Comparison between numerical and experimental results

The main characteristics of the finite element model were already described in the previous section.

In Figure 11 we compare the experimentally determined and FEA predicted equilibrium paths, while Figure 12 shows the finite element predicted deformed shapes for a pipe-arrestor system presenting a flattening cross-over mechanism.

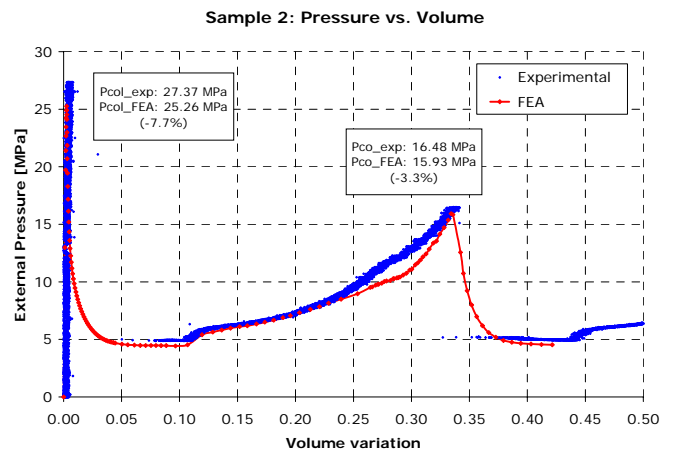


Figure 11. Sample 2; numerical vs. experimental results. Flattening mode.

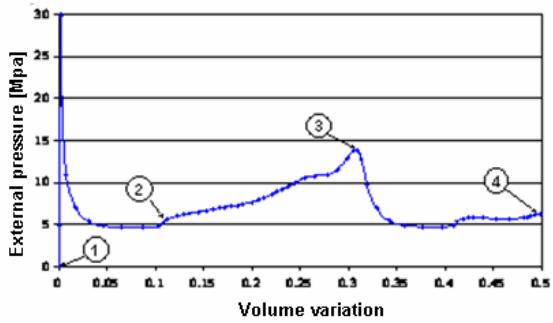
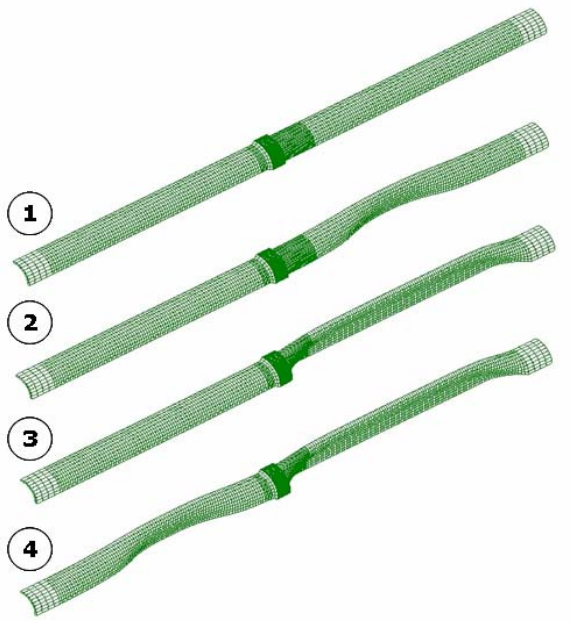


Figure 12. Sample 1; flattening cross-over mechanism

Figs. 13 and 14 present the results for sample 3, which collapses with a flipping mode.

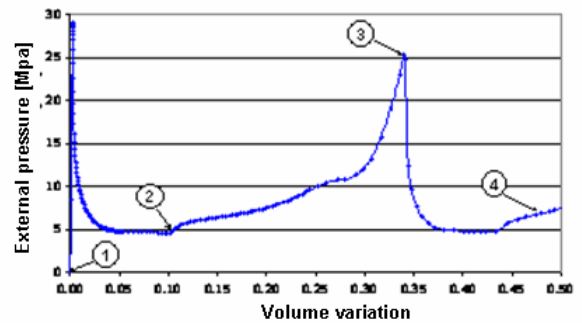
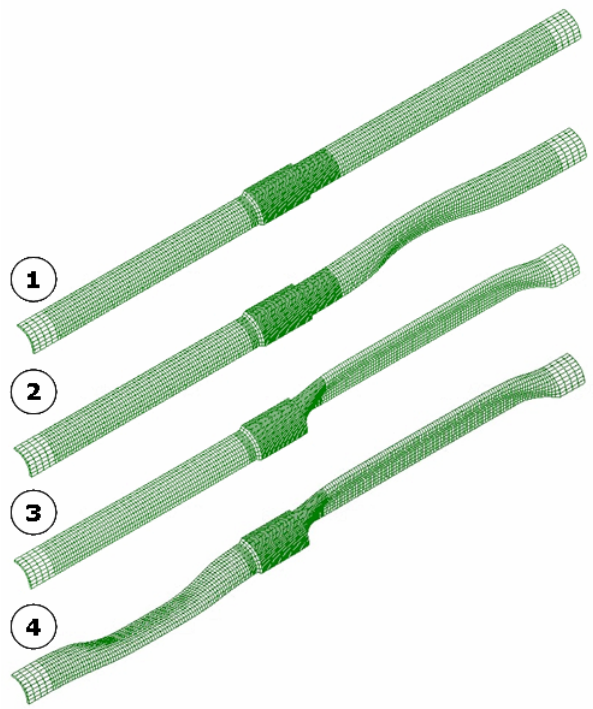


Figure 14. Sample 3; flipping cross-over mechanism

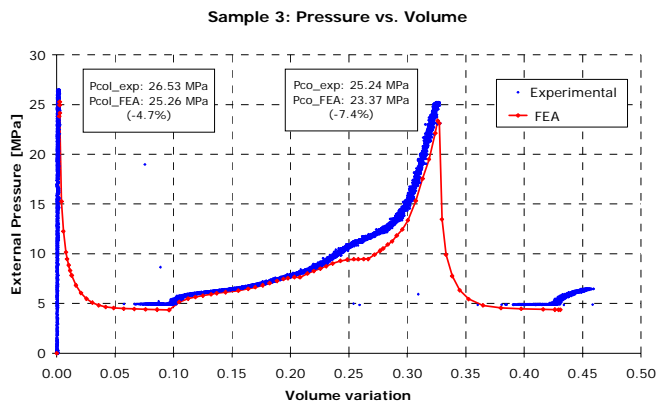


Figure 13. Sample 3; numerical vs. experimental results. Flipping mode.

Regarding Figs. 12 and 14, Point 1 is the unstrained initial condition and the point with maximum external pressure is the collapse point. At Point 2 the contact between opposite points on the pipe inner surface is established. Point 3 is the cross-over pressure. Finally, after the cross-over, the pressure decreases again, and collapse propagates (Point 4).

Finally in Figs. 15 and 16 we compare the experimentally observed and FEA predicted shapes of collapsed pipes after cross-over.



Figure 15. Sample 2. Flattening mode.

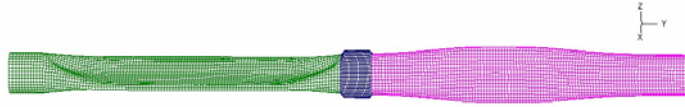


Figure 16. Sample 3. Flipping mode.

Table 4 compares the FEA results with the experimental ones:

| Sample | Collapse pressure: FEA/lab | Cross-over pressure: FEA/lab |
|--------|-------------------------------|---------------------------------|
| 1 | 0.921 | 1.006 |
| 2 | 0.923 | 0.967 |
| 3 | 0.953 | 0.927 |
| 4 | 0.859 | 0.910 |

Table 4. FEA vs. Experimental results

It is important to point out that the finite element results indicated in the previous table were obtained considering that the residual stresses in the two pipe sections are the residual stresses measured in the full length pipe. The modifications in residual stresses induced by the pipe cutting, the welding and groove machining were not considered in the model, this results in numerically predicted collapse pressures lower than the actual ones

PARAMETRIC ANALYSES

Parametric study of the arrestor cross-over pressure

As the agreement between the finite element predictions and the experimental results is very good, the finite element model can be used as a reliable engineering tool for analyzing the effect of different parameters on crossover pressure such as the arrestor thickness (h) and the arrestor length (L_a).

We selected as a base case a pipe reported by Mansour and Tassoulas [20] based on an experimental work previously done by Langner [16, 21]

The main characteristics of the pipe considered in the following analyses are:

Outer Diameter (D) = 323.85 mm. (12.75 in.)
 Thickness (t) = 15.875 mm.
 $D/t = 20.4$
 Material: X-52 steel, $E = 200.1$ Gpa [29900 ksi],
 $\sigma_y = 398.3$ MPa [15] and $E_t = 0.4\%$

The same material is employed for the arrestor.

A good measure of the arrestor effectiveness is the “arresting efficiency η ”, defined by Kyriakides [22] and given by:

$$\eta = \frac{P_{co} - P_p}{P_{col} - P_p} \quad 0 \leq \eta \leq 1$$

Where:

P_{col} : Collapse pressure of the pipe, referred to the downstream section.

P_p : Propagation pressure of the pipe.

P_{co} : Crossover pressure of the arrestor.

For all the following analysis, we consider external pressure only.

Variation of the arrestor thickness

As we increase the ratio between arrestor thickness (h) and pipe thickness (t), an increment of the value of the crossover pressure is observed and different structural behaviors are found. Figure 17 shows the variation of the efficiency with the arrestor thickness and Figure 18 the equilibrium path for some of the simulations.

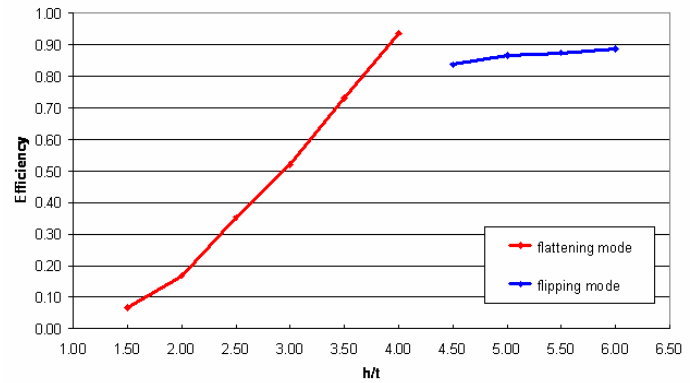


Figure 17. Efficiency vs. h/t ratio

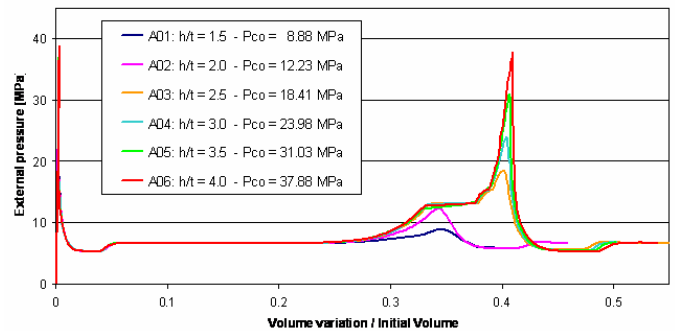


Figure 18: External Pressure vs. Internal volume variation for some simulations

Variation of the arrestor length

To study the dependence of the crossover pressure with the arrestor length we made two series of simulations with $h/t = 2.0$ and $h/t = 3.0$. The results are reported in Figures 19-21.

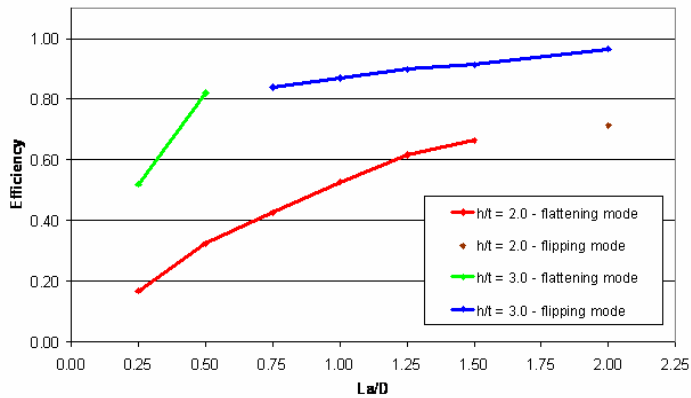


Figure 19: Efficiency vs. La/D ratio

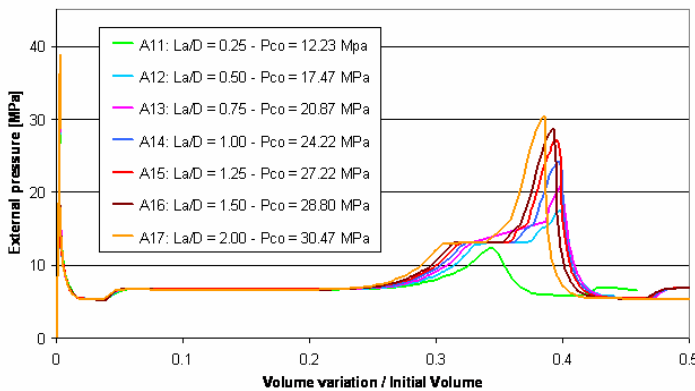


Figure 20: External Pressure vs. Internal volume variation for $h/t=2.0$.

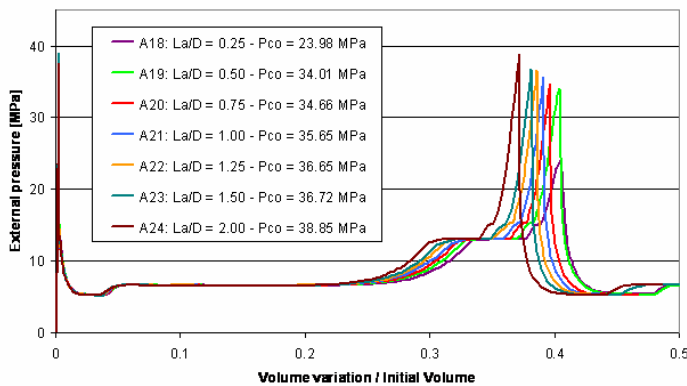


Figure 21: External Pressure vs. Internal volume variation for $h/t = 3.0$ arrestors

CONCLUSIONS

The agreement between the finite element predictions and the laboratory observations is excellent; hence, the developed finite element models can be used as reliable engineering tools for assessing on the collapse and post-collapse behavior of tubular products.

Regarding the buckle arrestors, a 3D finite element model was developed in order to be able to analyze the behavior of an integral ring buckle arrestor crossed over by a propagating buckle. The model was validated by comparing the numerical predictions with experimental determinations.

The model is able to simulate both, the flipping and the flattening cross-over mechanisms.

A parametric study varying the arrestor thickness, length and material hardening was carried out, showing that:

- The crossover pressure increases as arrestor became thicker, except in the transition between the flattening and the flipping mode.
- The crossover pressure increases with the arrestor length for the two h/t ratios considered ($h/t = 2.0$ and $h/t = 3.0$).

REFERENCES

- [1] Toscano, R.G., Timms, C., Dvorkin, E. and DeGeer, D., 2003, "Determination of the collapse and propagation pressure of ultra-deepwater pipelines", Proceedings OMAE 2003 - 22nd. International Conference on Offshore Mechanics and Arctic Engineering.
- [2] Park T. D. and Kyriakides S., 1997, "On the performance of Integral Buckle Arrestors for Offshore Pipelines", International Journal of Mechanical Sciences, Vol.39 pp.643-669.
- [3] Assanelli, A. P., Toscano, R.G., Johnson, D.H. and Dvorkin, E.N., 2000, "Experimental / numerical analysis of the collapse behavior of steel pipes", Engng. Computations, 17, pp.459-486.
- [4] Toscano, R. G., Gonzalez M. and Dvorkin E.N., 2003, "Validation of a finite element model that simulates the behavior of steel pipes under external pressure", The Journal of Pipeline Integrity, 2, pp. 74-84.
- [5] Toscano, R.G., Mantovano, L. and Dvorkin, E.N., 2004, "On the numerical calculation of collapse and collapse propagation pressure of steel deep water pipelines under external pressure and bending: Experimental verification of the finite element results", Proceedings 4th. International Conference on Pipeline Technology, pp. 1417-1428, Ostend, Belgium.
- [6] Toscano, R. G., Mantovano, L., Assanelli, A.P., Amenta, P., Johnson, D., Charreau, R. and Dvorkin, E. N., 2005, "Collapse arrestors for deepwater pipelines: Identification of crossover mechanisms", Rio Pipeline Conference and Exposition 2005, Technical Papers (paper IBP1021_05), Rio de Janeiro, Brazil.
- [7] Palmer, A.C. and Martin, J.H., 1975, "Buckle propagation in submarine pipelines", Nature, 254, pp. 46-48.
- [8] The ADINA SYSTEM, ADINA R&D, Watertown, MA, U.S.A.
- [9] Assanelli, A. P. and López Turconi, G., 2001, "Effect of measurement procedures on estimating geometrical parameters of pipes", 2001 Offshore Technology Conference, Paper OTC 13051, Houston, Texas.
- [10] Bathe, K. J., 1996, Finite Element Procedures, Prentice Hall, NJ.
- [11] Dvorkin, E. N. and Bathe, K. J., 1984, "A continuum mechanics based four-node shell element for general nonlinear analysis", Engng. Computations, 1, pp. 77-88.
- [12] Bathe, K.J. and Dvorkin, E. N., 1985, "A four-node plate bending element based on Mindlin / Reissner plate theory and a mixed interpolation", Int. J. Numerical Methods in Engng, 21, pp. 367-383.
- [13] Bathe, K.J. and Dvorkin, E. N., 1986, "A formulation of general shell elements - the use of mixed interpolation

of tensorial components”, *Int. J. Numerical Methods in Engng*, 22, pp.697-722.

- [14] Bathe, K.J. and Dvorkin, E. N., 1983, “On the automatic solution of nonlinear finite element equations”, *Computers & Structures*, 17, pp.871-879.
- [15] Johns, T. G., Mesloh, R. E. and Sorenson, J. E., 1978, “Propagating buckle arrestors for offshore pipelines”. *ASME Journal of Pressure Vessel Technology*, 100, pp. 206-214.
- [16] Langer, C. G., 1999, “Buckle arrestors for Deepwater Pipelines”, *Proceedings of the Offshore Technology Conference, OTC 10711, Houston, TX, U.S.A.*
- [17] Kyriakides, S., Park, T. D. and Netto, T. A., 1998, "On the design of Integral Buckle Arrestors for Offshore Pipelines", *International Journal of Applied Ocean Research*, 20 pp.95-104.
- [18] Netto, T. A. and Kyriakides, S., 2000, “Dynamic performance of integral buckle arrestors for offshore pipelines. Part I: Experiments”, *International Journal of Mechanical Sciences*, 42 pp.1405-1423.
- [19] Netto, T.A. and S.F. Estefen, “Buckle Arrestors for Deepwater Pipelines”, *International Journal of Marine Structures*, 9 pp.873-883, 1996
- [20] Mansour G.N. and Tassoulas J., “Analysis of the integral-ring arrestor for deep-water pipelines”, *Offshore Technology Research Center Texas A&M University*, 1995
- [21] Langner, C.G., "Arrest of Propagating Collapse Failures in Offshore Pipelines," part of "Deep-Water Pipeline Feasibility Study," Joint Industries Program 1973-1976, 42 Industry Sponsors, Shell Development Company.
- [22] Park, T.D. and Kyriakides, S., 1980, "On the “Slip On” Buckle Arrestors for Offshore Pipelines", *ASME Journal of Pressure Vessel Technology*, Vol.102 pp.188-193.